QSAR and 3D-QSAR of Phenothiazine Type Multidrug Resistance Modulators in P388/ADR Cells

Ivanka M. Tsakovska*

Centre of Biomedical Engineering, Bulgarian Academy of Sciences, Acad. G. Bonchev Str., Bl. 105, 1113 Sofia, Bulgaria

Abstract—A series of 25 phenothiazines and structurally related compounds was investigated by QSAR (quantitative structure activity relationship) and 3D-QSAR methods with respect to their MDR (multidrug resistance) reversing activity in P388/ADR-murine leukemia cell line resistant to ADR (adriamycin). The objective was to outline structural properties important for the investigated activity. Different measures for MDR reversal were used and compared. Two 3D-QSAR approaches were applied—CoMFA (comparative molecular field analysis) and CoMSIA (comparative molecular similarity indices analysis). Both, neutral and protonated forms of the compounds were investigated. Molecular models with good predictive power were derived using a hydrophobic field alone and a combination of steric, hydrophobic, and hydrogen bond acceptor fields of the compounds. In the combined models highest contribution of the hydrogen bond acceptor field was noticed. Thus, the dominant role of the hydrophobic and hydrogen bond acceptor fields for MDR reversing activity of the investigated compounds was demonstrated. The structural regions responsible for the differences in anti-MDR activity were analyzed in respect to their hydrophobic, hydrogen bond acceptor and steric nature. The results may direct design of new phenothiazines and related compounds as MDR modulators.
© 2003 Elsevier Science Ltd. All rights reserved.

Introduction

Multidrug resistance (MDR) is a major problem in cancer chemotherapy. Usually it is multifactorial, i.e., multiple mechanisms of resistance can act in the same resistant cell. The drug efflux caused by the transmembrane transport P-glycoprotein (Pgp) is one of the most studied and widespread mechanisms of MDR in tumor cells.[1] A large number of pharmacological agents have been identified to reverse MDR. They are suggested to block the anticancer drug transport by binding either to the drug's interaction site (competitive inhibition) or to other binding site, leading to allosteric inhibition of the drug outward transport.[2] The MDR modulators are chemically and structurally different compounds. In general, they are not cytotoxic and vary widely in their main biological action - calcium channel blockers, neuroleptics, antidepressants, steroid hormones, etc.[3–5] Many investigations have been undertaken to find out common structural features responsible for recognition of the compound by Pgp. Knowledge compiled from various structure–activity studies directs to the fact that

hydrophobicity of a molecule is important for the interaction with Pgp. Because aromatic groups largely contribute to the hydrophobicity, planar ring structures seem to be characteristic of anti-MDR activity. Presence of a basic nitrogen atom in an aliphatic chain attached to the aromatic structure also seems to play an important role for the interaction with Pgp.[6] Additionally, presence of a hydrogen bond acceptor near the aromatic ring system is outlined as an important feature of active modulators.[7,8]

Phenothiazines and structurally related compounds are among the most studied MDR modulators. Their MDR reversing activity has been assessed in different resistant tumor cell lines and several structure–activity relationships have been derived. Studies of Ford et al.[9,10] indicate that -CF$_3$ or -Cl at position 2 in the nucleus, a para-methyl substituted piperazinyl side chain, and a four-carbon bridge between these two domains are optimum for MDR reversing activity. In general, thioxanthene derivatives are more hydrophobic (higher octanol/buffer partition coefficient) than the corresponding phenothiazine derivatives and also more potent. Ramu et al.[11,12] point to the positive role of the carbonyl group, regardless of its molecular location. The first QSAR and 3D-QSAR models of phenothiazines and related

*Tel.: +359-2-9793605; fax: +359-2-723787; e-mail: itsakovska@clbme.bas.bg

compounds are described in the studies of Pajeva and Wiese[13,14] using phenothiazines and structurally related compounds with MDR reversing activity estimated in ADR (adriamycin) resistant MCF-7/ADR cell line. Anti-MDR activity as defined by Ford[9,10] (IC_{50} of ADR alone, divided by IC_{50} of ADR plus the modifying drug at a subinhibitory concentration ($\leq IC_{10}$)) is used. The QSAR contributing features confirm the empirical results of Ford et al.[9,10] However, the 3D-QSARs point to key role of hydrophobicity as a 3D directed molecular property for MDR reversal.

In the present study structural characteristics of phenothiazines and structurally related MDR modulators were evaluated in the ADR resistant murine leukemia cell line, P388/ADR.[12] Different measures for MDR reversing activity were used. QSAR and two 3D-QSAR approaches–comparative molecular field analysis (CoMFA) and comparative molecular similarity indices analysis (CoMSIA) were applied. The neutral and protonated forms were analyzed. Models with good predictive power were obtained with hydrophobic, hydrogen bond acceptor and steric fields outlining in this way the dominant role of these fields for MDR reversing activity of the studied modulators.

Results

A representative set of 25 phenothiazines and structurally related compounds was chosen from the large set tested by Ramu and coworkers.[12] The compounds were selected to have a common parental structure and to range in biological activity by more than two log units so that to reduce the risk of chance correlations. The activity parameters as evaluated in P388 sensitive and ADR resistant murine leukemia cell line were used:

$$A = ED_{50 \text{ compound P388}}, \quad \mu M;$$

$$B = ED_{50 \text{ compound P388/ADR}}, \quad \mu M;$$

$$C = \frac{ED_{50 \text{ compound P388/ADR}}}{ED_{50(\text{compound}+0.2\,\mu M \text{ ADR})P388/ADR}}$$

According to the reference [12] A and B represent cytotoxicity of the compounds in the sensitive and resistant cell line respectively, C reflects the ability of the compounds to reverse MDR. ED_{50} of the compounds measured in the presence of $0.2\,\mu M$ ADR was calculated from C. This effect (coded ED in the study) appears as another measure of MDR reversing activity. In the study the values of the above parameters were transformed to logarithmic scale. The inverse values of A, B and ED were used to obtain higher values for the more active compounds. The monoprotonated forms were built and investigated considering that the basic tertiary nitrogen in the aliphatic chain is highly protonated at physiological pH. As there were structures with two nitrogen atoms in the aliphatic chains, the decision about the right protonated nitrogen was taken on the basis of pKa values. Table 1 contains the names, structures, biological parameters and pKa values of the studied compounds.

First, the correlations between the biological parameters were investigated. The results showed strong correlation between cytotoxicity of the modulators alone in the sensitive (A) and the resistant cell line (B) (eq 1).

$$lg(1/B) = 0.850(\pm 0.055)lg(1/A) - 0.313(\pm 0.070)$$
$$n = 25 \quad R^2 = 0.911 \quad SEE = 0.104 \quad F = 235.18 \quad (1)$$

This suggests that the same cytotoxic mechanism is acting in both cell lines and the observed shift in the line can be related to a different, presumably MDR-related mechanism. The correlations of C with A and B were also studied:

$$lgC = 1.461(\pm 0.210) + 0.521(\pm 0.167)lg(1/A)$$
$$n = 25 \quad R^2 = 0.297 \quad SEE = 0.313 \quad F = 9.732 \quad (2)$$

$$lgC = 1.584(\pm 0.262) + 0.561(\pm 0.190)lg(1/B)$$
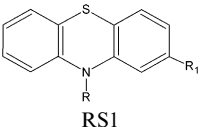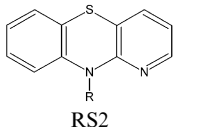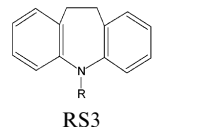$$n = 25 \quad R^2 = 0.274 \quad SEE = 0.319 \quad F = 8.673 \quad (3)$$
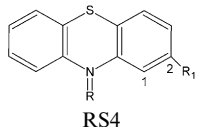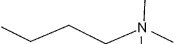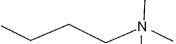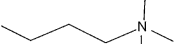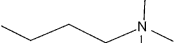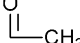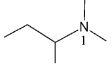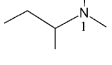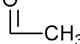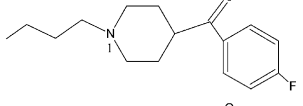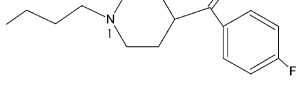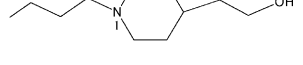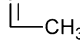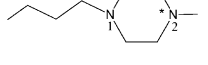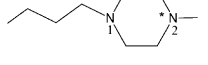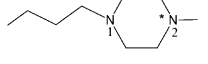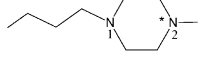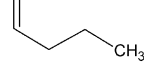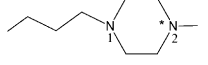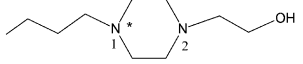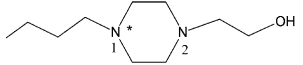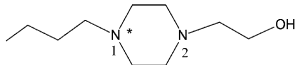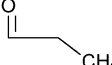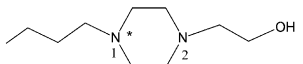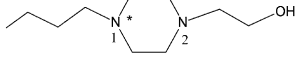
Much worse correlations were observed. As C is a ratio between own cytotoxicity of the modulator in the resistant cell line (B) and cytotoxicity of the modulator in the presence of ADR (ED), the lack of linear correlation can be due to ED, suggesting its possible use as another measure of the modulators' ability to overcome MDR.

Five types of indicator variables were considered in the Free–Wilson analysis:

- A type of the ring system: RS1, RS2, RS3 and RS4 as designated in Table 1.
- A substituent on the 2nd position in the ring system (R1): R11 = –H; R12 = –Cl; R13 = –CF$_3$; R14 = –COC$_n$H$_{2n+1}$ (n = 2, 3); R15 = –COCH$_3$; R16 = –SO$_2$N(CH$_3$)$_2$.
- A type of the aliphatic chain between the ring system and the first tertiary nitrogen: Alk, normal; Iprp, isopropyl; Ibut, isobutyl.
- A type of the tertiary nitrogen in the side chain: N$_{Alk}$, alkyl substituted; N$_{Prd}$, belonging to a piperidine moiety; N$_{Prz}$, belonging to a piperazine moiety.
- A substituent at the tertiary nitrogen in the aliphatic chain (R): R1 = –CH$_3$; R2 = –COC$_6$H$_4$F; R3 = –CH$_2$CH$_2$OH.

As a reference structure the low active compound promazine (RS1, R11, Alk, N$_{Alk}$, R1) was taken. Several runs were performed and the final regression equations included only structural variables that were statistically significant compared to the reference (p-level ≤ 0.05). The models are shown by eq 4 (dependent variable lgC) and eq 5 (dependent variable lg(1/ED)).

Table 1. Activity data for the compounds studied

RS1   RS2   RS3   RS4

Compound	R	R_1	lg(1/A)	lg(1/B)	lg$C$	lg(1/ED)	pKa_1	pKa_2
RS1								
1. Promazine			−1.602	−1.778	0.477	−1.301	9.43	—
2. Chlorpromazine		Cl	−1.079	−1.301	0.398	−0.903	9.41	—
3. Triflupromazine		CF_3	−1.079	−1.301	0.398	−0.903	9.40	—
4. Acepromazine		$O\!=\!C\text{-}CH_3$	−1.477	−1.653	0.748	−0.905	9.41	—
5. Promethazine			−1.778	−1.778	0.875	−0.903	8.98	—
6. Acepromethazine		$O\!=\!C\text{-}CH_3$	−1.602	−1.903	0.778	−1.125	8.93	—
7. Duoperone		CF_3	−1.000	−1.079	1.427	0.347	8.41	—
8. AHR 06601		$O\!=\!C\text{-}CH_3$	−1.000	−1.079	1.301	0.222	8.42	—
9. Piperacetazine		$O\!=\!C\text{-}CH_3$	−1.301	−1.301	0.643	−0.658	9.38	—
10. Perazine			−1.079	−1.301	0.643	−0.658	4.07	7.82
11. Prochlorperazine		Cl	−0.653	−0.903	0.826	−0.077	4.04	7.82
12. Trifluoperazine		CF_3	−0.653	−0.903	1.000	0.097	4.04	7.81
13. Butaperazine		$O\!=\!C\text{-}CH_2\text{-}CH_3$	−0.653	−0.903	1.250	0.347	4.04	7.82
14. Thioproperazine		$SO_2N(CH_3)_2$	−0.903	−1.301	1.223	−0.078	4.03	7.81
15. Perfenazine		Cl	−0.903	−1.000	0.699	−0.301	7.22	3.43
16. Acetophenazine		$O\!=\!C\text{-}CH_3$	−1.176	−1.301	1.000	−0.301	7.22	3.43
17. Carphenazine		$O\!=\!C\text{-}CH_2\text{-}CH_3$	−1.079	−1.079	1.176	0.097	7.22	3.43
18. Fluphenazine		CF_3	−0.903	−0.903	0.602	−0.301	7.21	3.43
RS2								
19. Oxypendyl			−1.778	−1.778	0.301	−1.477	7.18	3.43

2892

I. M. Tsakovska / Bioorg. Med. Chem. 11 (2003) 2889–2899

Table 1 (*continued*)

Compound	R	R_1	lg(1/A)	lg(1/B)	lgC	lg(1/ED)	pKa$_1$	pKa$_2$
20. Prothipendyl			−1.778	−1.778	0.114	−1.664	9.37	—
RS3 21. Imipramine			−1.778	−1.778	0.477	−1.301	9.49	—
22. Trimipramine			−1.778	−1.778	0.778	−1.000	9.38	—
RS4 23. *cis*-Thiothixene		$SO_2N(CH_3)_2$	−1.079	−1.301	1.398	0.097	3.47	7.73
24. Clopenthixol		Cl	−1.000	−1.079	1.176	0.097	6.92	3.38
25. *cis*-Flupenthixol		CF_3	−0.903	−1.079	1.176	0.097	6.92	3.39

1, 2 - numbering of the nitrogen atoms corresponds to the calculated pKa values.
*Nitrogen atom likely to be protonated at physiological pH.

$$lg\ C = 0.619(\pm 0.052) + 0.417(\pm 0.131)R14 - 0.500$$
$$\times (\pm 0.122)RS2 + 0.454(\pm 0.113)RS4$$
$$+ 0.177(\pm 0.080)N_{Prz} + 0.745(\pm 0.126)R2 \quad (4)$$
$$n = 24 \quad R^2 = 0.847 \quad SEE = 0.162 \quad F = 19.861$$

$$lg(1/ED) = 0.490(\pm 0.172)R14 - 0.951$$
$$\times (\pm 0.163)RS2 + 0.365(\pm 0.148)RS4$$
$$+ 0.703(\pm 0.103)N_{Prz} + 1.256 \quad (5)$$
$$\times (\pm 0.169)R2 - 0.971(\pm 0.070)$$
$$n = 25 \quad R^2 = 0.903 \quad SEE = 0.217 \quad F = 35.176$$

The number of the compounds included in the first model (eq 4) was 24 because thioproperazine was evaluated as an outlier in the analysis. The analysis of the structural variety revealed that thioproperazine had relatively unique structure—$SO_2N(CH_3)_2$ substituent on the 2nd position in the ring system could be found only in one more compound—*cis*-thiothixene, an active thioxanthene. The remaining part of the structure resembled the structure of relatively low active phenothiazines (**10**, **11**, **12** in Table 1). As a result biological

activity of thioproperazine was underestimated and it was evaluated as an outlier in the analysis.

Both models (eqs 4 and 5) outlined one and the same structural features responsible for MDR reversal but the statistical significance of the second one (eq 5) was slightly higher. In Figure 1 predicted versus observed lg(1/ED) values obtained by eq 5 are presented. In the figure the number of the points is less because some of the compounds had equal experimental lg(1/ED) and calculated lg(1/ED) values resulting in the same point (compounds **1** and **21**; **2**, **3**, **4** and **5**; **11** and **14**; **15**,**16** and **18**; **23**, **24** and **25** in Table 1). Clusters of points resulted from predicting the same lg(1/ED) value for compounds with different observed lg(1/ED). The first cluster included compounds **1**, **2**, **3**, **4**, **5**, **6**, **9**, **21**, **22** (Table 1) with predicted lg(1/ED) = −0.971. They had no structural features significantly contributing to anti-MDR activity that is why predicted activity was equal to the intercept of the eq 5. The other cluster (predicted lg(1/ED) = −0.268) included compounds **10**, **11**, **12**, **14**, **15**, **16**, **18** (Table 1). They all contained piperazine nitrogen-significant for the MDR reversal according to the Free–Wilson model (eq 5). Thus, despite the statistically significant Free–Wilson models the observed clustering revealed that the selected features did not allow us to precisely differentiate between the compounds' activities. To find out such parameters 3D-QSAR was performed by CoMFA and CoMSIA. Both measures of MDR reversing activity were studied. Better 3D-QSAR models were obtained with lg (1/ED) in comparison with lgC values therefore ED was considered in the presented 3D-QSAR analyses.
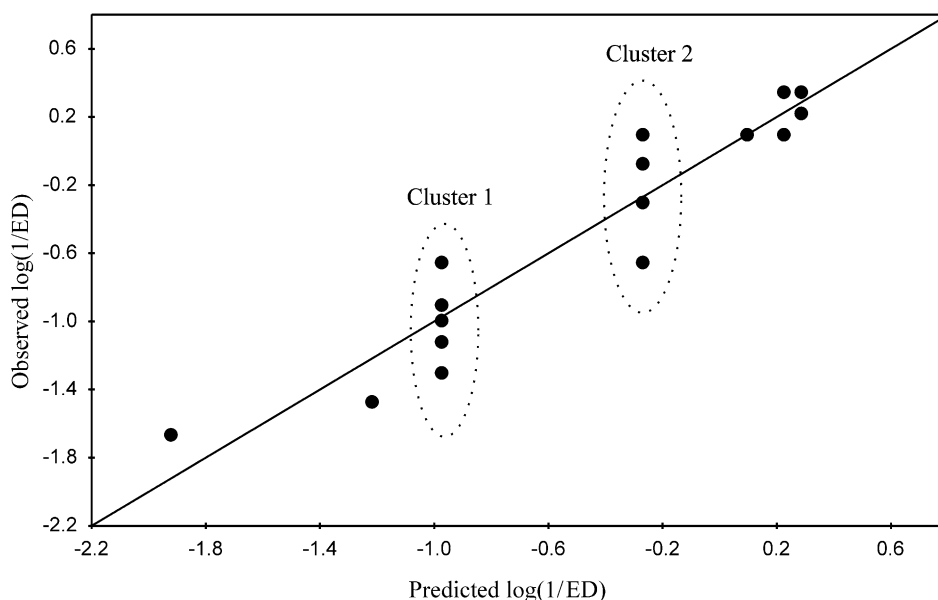
Figure 1. Predicted versus observed log (1/ED) values according to eq 5.

First, the cross-validated models were obtained with all compounds—neutral and protonated forms (Table 2). The CoMFA and CoMSIA models revealed similar results.

Next, the compounds were divided into a training and a test set. The test set was formed by grouping the compounds according to their anti-MDR activity into low and high active group and subsequent random selection of three compounds from each group. The rest of the compounds formed the training set. The procedure was repeated several times and similar CoMFA and CoMSIA results were obtained for the selected training sets. The models obtained by random selection of **1**, **2**, **10**, **12**, **13**, and **16** as test compounds, are given in Table 3.

Table 4 represents non-cross-validated models and predictive Q_{pr}^2 of the best crossvalidated models. The analysis of the Q_{pr}^2 values showed that the obtained models had good external predictive power.

The graph of predicted versus observed anti-MDR activity by the CoMSIA model with steric, hydrophobic and acceptor fields (Table 4) is given in Figure 2.

The results show highest Q_{cv}^2 for the models with hydrophobic fields and a combination of hydrophobic, acceptor and steric fields. To evaluate the structural areas where these fields have highest contributions to anti-MDR activity, the STDEV*COEFF contour plots were built (Figs. 3–5). The coloured regions correspond to differences in the fields which contribute mostly (about 80% of the signal) to the differences in investigated activity. In Figure 3 the regions where more hydrophobicity is necessary for higher anti-MDR activity are given in blue and regions where more hydrophilicity

Table 2. CoMFA and CoMSIA models using all compounds in neutral and protonated forms (alignment 1 and alignment 2): the models with highest predictive ability are given in bold

Field	Neutral forms alignment	Protonated forms (alignment 1)	Protonated forms (alignment 2)
	$Q_{cv}^2/N_{opt}/SEP$	$Q_{cv}^2/N_{opt}/SEP$	$Q_{cv}^2/N_{cv}/SEP$
CoMFA			
Steric	**0.768/5/0.334**	**0.716/6/0.380**	0.567/3/0.434
Electrostatic	0.618/4/0.418	0.620/2/0.397	0.601/2/0.408
Both	0.736/6/0.366	0.693/2/0.357	0.572/3/0.432
CoMSIA			
Steric	0.713/2/0.346	0.708/3/0.356	0.589/4/0.434
Electrostatic	0.587/3/0.424	0.571/5/0.455	0.602/5/0.438
Steric + electrostatic	0.690/6/0.397	0.669/3/0.380	0.629/3/0.402
Hydrophobic	**0.795/4/0.306**	**0.784/4/0.314**	**0.710/5/0.374**
Donor	0.019/4/0.670	0.517/6/0.495	0.550/5/0.466
Acceptor	0.656/5/0.404	0.671/7/0.421	0.498/7/0.520
Donor + acceptor	0.594/6/0.454	0.708/7/0.396	0.560/5/0.460
Steric + hydrophobic	**0.827/5/0.289**	**0.828/4/0.280**	**0.720/5/0.367**
Steric + acceptor	**0.796/6/0.322**	**0.761/7/0.359**	**0.660/5/0.405**
Hydrophobic + acceptor	**0.844/5/0.274**	**0.809/6/0.311**	**0.710/5/0.374**
Steric + hydrophobic + acceptor	**0.850/4/0.262**	**0.834/6/0.290**	**0.707/6/0.386**

Table 3. CoMFA and CoMSIA models using training set compounds in neutral and protonated forms (alignment 1): the models with highest predictive ability are given in bold

Field	Neutral forms alignment			Protonated forms (alignment 1)		
	Q^2_{cv}	N_{opt}	SEP	Q^2_{cv}	N_{opt}	SEP
CoMFA						
Steric	0.715	2	0.358	0.628	2	0.409
Electrostatic	0.504	4	0.505	0.572	2	0.439
Both	0.712	2	0.360	0.691	2	0.373
CoMSIA						
Steric	0.728	2	0.350	**0.700**	**2**	**0.368**
Electrostatic	0.576	5	0.485	0.538	3	0.471
Steric + electrostatic	0.685	3	0.389	0.652	3	0.409
Hydrophobic	**0.845**	**5**	**0.293**	**0.777**	**4**	**0.338**
Donor	0.060	5	0.722	0.556	8	0.565
Acceptor	0.632	5	0.451	0.528	5	0.512
Donor + acceptor	0.578	8	0.551	0.675	6	0.442
Steric + hydrophobic	**0.804**	**4**	**0.317**	**0.740**	**4**	**0.366**
Steric + acceptor	**0.760**	**5**	**0.322**	0.690	5	0.414
Hydrophobic + acceptor	**0.813**	**5**	**0.322**	**0.761**	**5**	**0.364**
Steric + hydrophobic + acceptor	**0.816**	**4**	**0.307**	**0.766**	**5**	**0.360**

Table 4. Non-crossvalidated models and Q^2_{pr} of the best CoMSIA crossvalidated models

Field	Neutral forms alignment				
	$R^2/SEE/F_{ratio}$	Fraction			Q^2_{pr}
		Steric	Hydrophobic	Acceptor	
Hydrophobic	0.989/0.078/236.864	—	1	—	0.725
Steric + hydrophobic	0.970/0.125/112.636	0.297	0.703	—	0.767
Steric + acceptor	0.969/0.131/81.436	0.295	—	0.705	0.663
Hydrophobic + acceptor	0.988/0.083/208.125	—	0.442	0.558	0.805
Steric + hydrophobic + acceptor	0.977/0.109/149.457	0.149	0.378	0.473	0.749
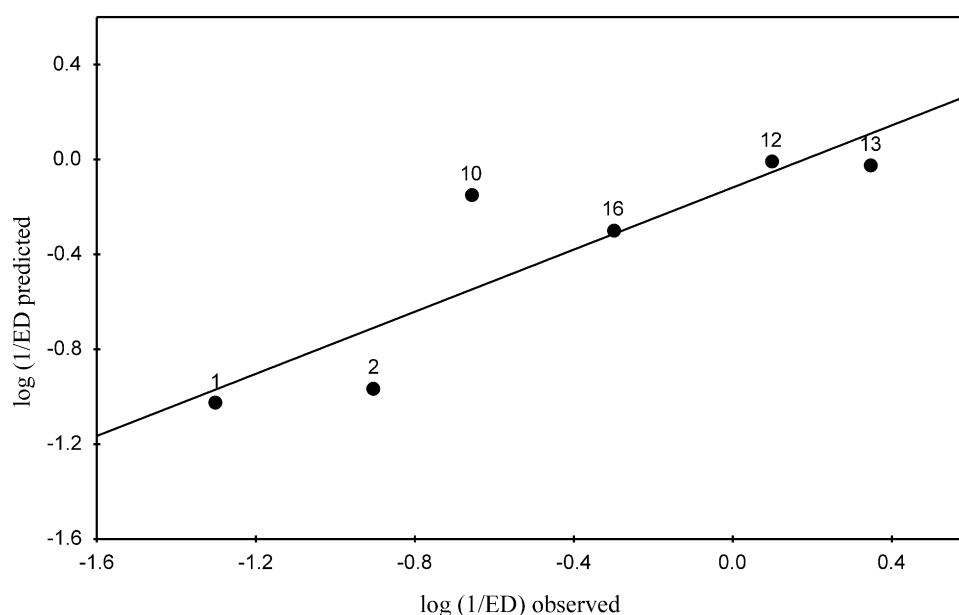
Figure 2. Predicted log (1/ED) values of the test compounds obtained by steric + hydrophobic + acceptor field CoMSIA model versus observed log (1/ED): $n = 6$; $R^2 = 0.858$; $F = 30.231$; $SEE = 0.245$.

I. M. Tsakovska / Bioorg. Med. Chem. 11 (2003) 2889–2899

2895

favours activity are given in red. In Figure 4 the blue regions correspond to hydrogen bond donor groups of the receptor that participate in favourable interactions with the ligands. Conversely, the red regions indicate hydrogen bond donor groups of the receptor unfavorable for the interactions with the ligands. The sterically important regions are given in blue and respectively the sterically forbidden ones are given in red (Fig. 5). The contouring levels of the positive and negative regions in the plots were selected keeping the same ratio between the contributions of the extreme positive and negative terms as between the positive and negative terms in the whole field.[15]

Discussion

The compounds selected in the present study had the same parent skeleton. Thus, the most important
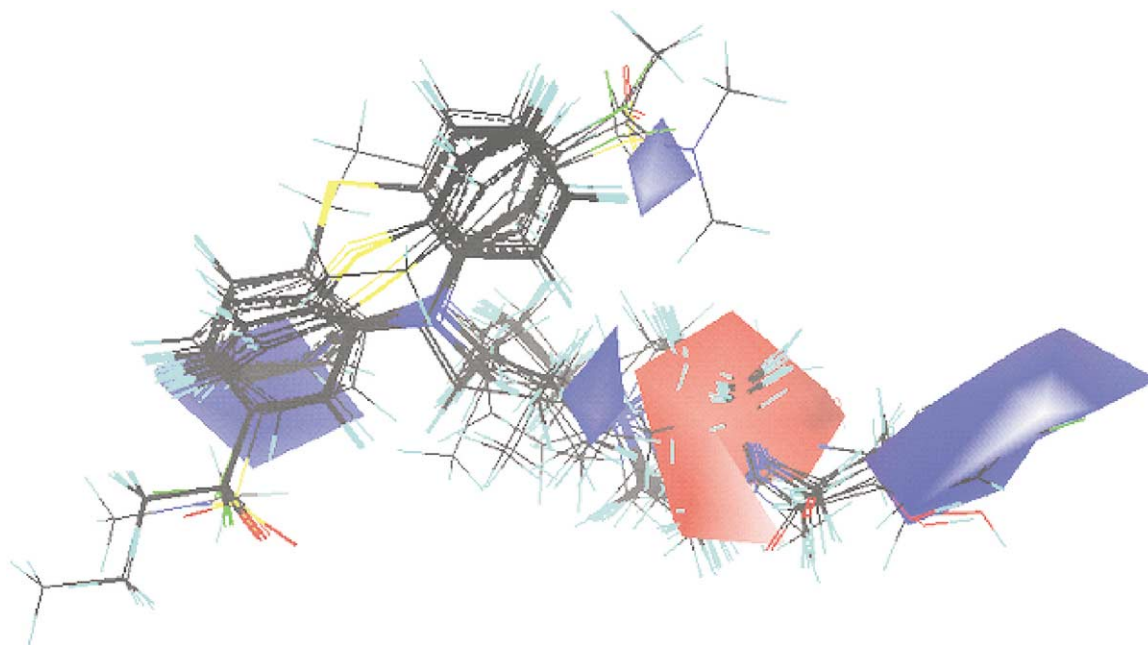
Figure 3. CoMSIA STDEV*COEFF contour plot of hydrophobic field: the blue contours indicate regions in the molecules where higher hydrophobicity favors anti-MDR activity and the red contours indicate regions in the molecules where higher hydrophilicity favors anti-MDR activity.

Figure 4. CoMSIA STDEV*COEFF contour plot of hydrogen bond acceptor field: the blue contours indicate regions on the receptor where hydrogen bond donor groups are mostly likely located and the red contours indicate regions on the receptor where hydrogen bond donor groups should be absent.
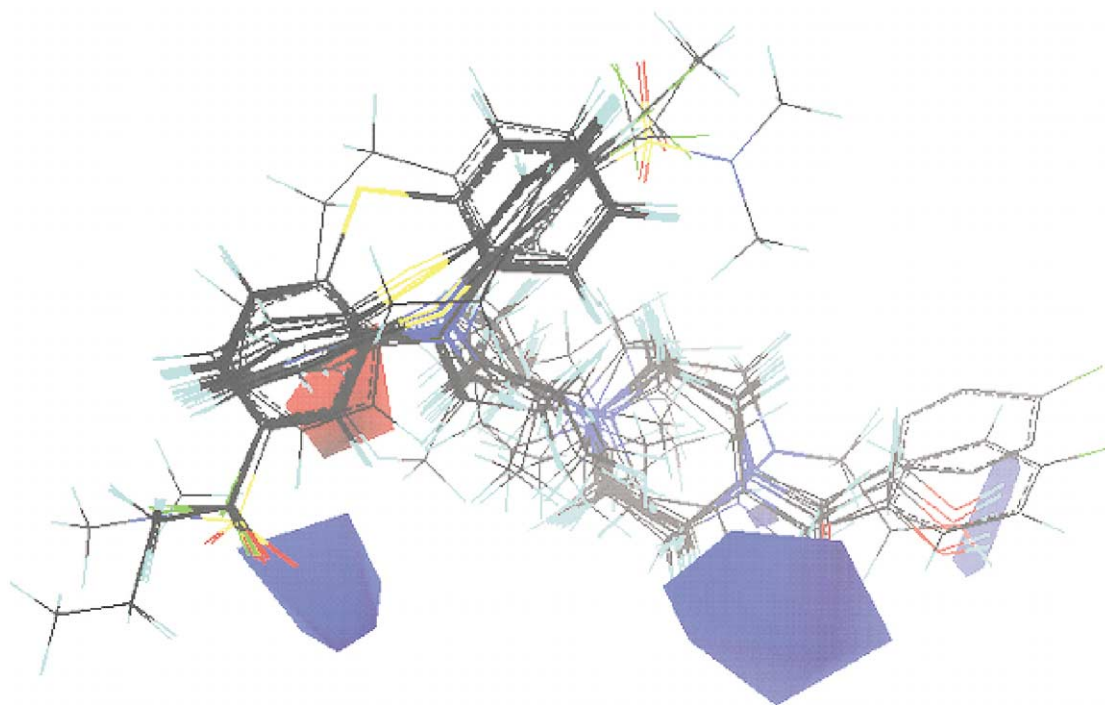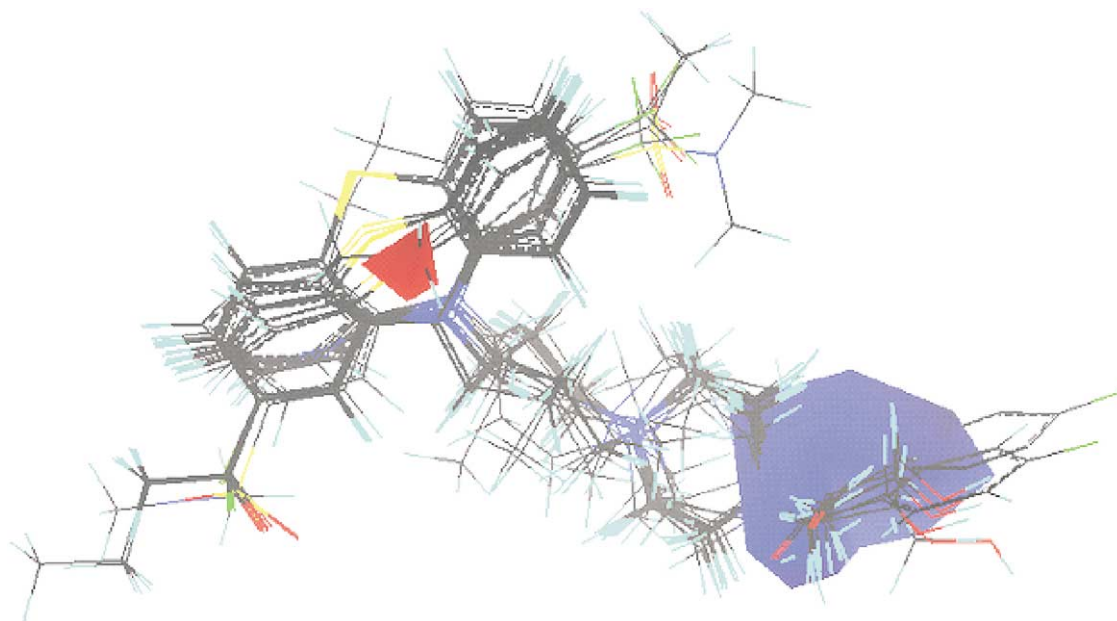
Figure 5. CoMSIA STDEV*COEFF contour plot of steric field: the blue contour indicates sterically favorable region in the molecules and the red contour indicates sterically forbidden region in the molecules.

prerequisite for successful application of the Free–Wilson analysis in drug design (congenericity within a series of compounds) was met. The obtained model (eq 5) evaluated the ring system RS4 (9H-thioxanthene) as a variable with a positive contribution and the ring system RS2 (10H-pyrido[3,2-b][1,4]benzothiazine) as a variable with a negative contribution to anti-MDR activity of the investigated compounds. This can be partially related to the hydrophobic nature of the ring system. Indeed, the $\log P$ values of the considered ring systems confirm this suggestion: $\log P$ (9H-thioxanthene) = 4.33 ± 0.26; $\log P$ (10H-pyrido[3,2-b][1,4]benzothiazine) = 2.80 ± 0.28). So one can conclude that presence of more lipophilic ring system is preferable for anti-MDR activity of the compounds studied. This is in agreement with previously reported results on phenothiazines and related drugs.[10,14] Additionally the following structural fragments were selected with positive contributions to anti-MDR activity of the compounds:

- R14, –COC$_n$H$_{2n+1}$ ($n = 2, 3$). This feature suggests two possibilities - influence of a long flexible aliphatic bridge or participation of the oxygen atom as a hydrogen bond acceptor.
- N_{Prz}, a tertiary nitrogen atom belonging to a piperazine moiety. It can function as a hydrogen bond acceptor or donor depending on the drug interacting form (neutral or protonated).
- R2, –COC$_6$H$_4$F. A possible interpretation of the role of this substituent follows from presence of a bulky phenyl ring that might be involved in steric and hydrophobic interactions with the receptor. Another interpretation implies the role of the carbonyl oxygen as a hydrogen bond acceptor in agreement with the suggestion of Ramu et al. about the role of the carbonyl group for the formation of intra- or intermolecular hydrogen bonds.[12]

The Free–Wilson model (eq 5) correlates well the MDR reversal activity in the investigated series of compounds. However, as shown in Results it is not able to differentiate between the structural features of some the investigated compounds. This is a general limitation of this approach and additional methods can be applied to overcome it. Tmej and coworkers, for example, have performed a combined Hansch/Free–Wilson approach using both physicochemical parameters and substructure related indicator variables for prediction of MDR reversal ability of propafenone type MDR modulators.[16] The presented here Free–Wilson analysis of phenothiazines and structurally related compounds is followed by 3D-QSAR analyses. Thus the role of the structural features identified by the Free–Wilson models is elucidated by getting insight into their spatial properties. Additionally, 3D-QSAR analyses reveal other spatial features responsible for anti-MDR activity of the studied compounds.

As seen from the hydrophobic field contour plot (Fig. 3) there are two regions in the vicinity of the ring system where more hydrophobicity is favorable. One is related to the substituent on the second position, and implies that it should be more lipophilic for higher anti-MDR activity. The other region relates to the one of the aromatic rings. Obviously 10H-pyrido[3,2-b][1,4]benzothiazine ring system which is nitrogen containing and, consequently, more hydrophilic is less favourable for high MDR modulating activity. This is in agreement with the Free–Wilson analysis' results (eq 5) where RS2, 10H-pyrido[3,2-b][1,4]benzothiazine contributes negatively to activity. In fact, oxypendyl and prothipendyl, the compounds possessing this type ring system have lowest anti-MDR activity (Table 1). 3D-QSAR analysis also explained the role of –COC$_6$H$_4$F substituent at the tertiary nitrogen in the aliphatic chain selected by the Free–Wilson analysis as important for the MDR reversal.

The blue region in the contour plot (Fig. 3) directs us to favourable hydrophobic interactions between this substituent and the receptor. Additionally the more hydrophobic aliphatic chain would also increase the activity. The well defined red signal (Fig. 3) is associated with the nitrogen atom in the aliphatic chain and indicates that more hydrophilic piperazine moiety is preferable. This result explains why the nitrogen belonging to the piperazine has a positive contribution to anti-MDR activity in the Free–Wilson model (eq 5).

The hydrogen bond acceptor field contour plot (Fig. 4) involves blue contours, indicating regions on the receptor where the presence of hydrogen bond donor groups is favourable for the binding. They are close to the carbonyl and hydroxyl groups in the substituent attached to the tertiary nitrogen in the aliphatic chain of the investigated compounds. That means that the presence of hydrogen bond acceptors is preferable in these positions. Favourable hydrogen bond acceptor group is registered also at the second position of the ring system. That is why $-COC_nH_{2n+1}$ and $-COC_6H_4F$ substituents are selected to have positive contributions to activity in the Free–Wilson analysis. The red contour reveals region of the receptor where hydrogen bond donor should be absent. Therefore for the compounds with RS2 type ring system (Table 1) the interaction of the nitrogen atom in the aromatic ring as a hydrogen bond acceptor is not favourable. This implies indirectly that the more lipophilic ring system, the higher MDR reversal can be expected.

The blue region in Figure 5 indicates preferable presence of a bulky substituent bound to the tertiary nitrogen in the aliphatic chain. The red (sterically forbidden) region in the cyclic system might be related to the more bulky imipramine ring system. In fact, imipramine and trimipramine are low active compounds.

The analyzed contour plots were built on the basis of the best 3D-QSAR models derived with hydrophobic field and combinations of hydrophobic, hydrogen bond acceptor and steric field. The role of hydrophobicity as a 3D directed molecular property for the anti-MDR activity of phenothiazines and structurally related compounds has been suggested in previous investigations.[14] In the same study it has been shown that the steric field also contribute significantly to the MDR reversal. The steric field has also been underlined in the study of Kim where substituted imidazoles had been investigated as MDR modulators and the best CoMFA and CoMSIA models had been derived with steric and electrostatic fields.[17] This investigation revealed that the highly predictive models also included hydrogen bond acceptor field. Moreover, in the combined fields' models (Table 4) the hydrogen bond acceptor field had the biggest fraction. This pointed to the important role of the hydrogen bond acceptor field together with the hydrophobic and steric ones for activity of phenothiazine type MDR modulators.

The discussed above models use MDR reversing activity measured in an animal cell line.[12] Although a different cell line and activity measures are used, the identified structural features important for MDR reversal are similar to those reported for human cell lines[13,14] pointing to similar mechanism of MDR reversal by the studied drugs.

As reviewed in the Introduction the basic nitrogen is supposed to have impact on activity of MDR modulators. However, it is not clear if its interaction with the receptor is ionic or not. According to Ecker and coworkers it is nonionic and determined by electron donor capability.[18] Models of Pgp functioning[19,20] suggest interaction between the drug and the protein binding site in the membrane that supposes involvement of the neutral form of the drug. In confirmation of the opposite hypothesis quaternary propafenone analogues has been identified as P-gp substrates.[21]

As it was not clear if the phenothiazines did àct as neutral or protonated, both were analyzed. Comparison between the spatial structures revealed very similar geometries of the neutral and charged forms (RMS values of the fit between the centroids of the aromatic rings and the first nitrogen atom in the aliphatic chain was in range 0.012–0.210). Analysis of the protonated forms in the CoMSIA models (Tables 2 and 3) revealed that the hydrogen bond donor field did not contribute significantly to anti-MDR activity. On the basis of the above considerations and the slightly better models obtained for the neutral forms (Tables 2 and 3) one can speculate that the neutral functional state of the investigated compounds is the preferable one for the studied activity.

Conclusion

In summary, 3D-QSAR models with moderate to high predictive ability of phenothiazine type MDR modulators were derived. The role of hydrophobicity as a 3D property was confirmed[14] and also hydrogen bond acceptor interactions were found to contribute to anti-MDR activity. The obtained models may help design of new active phenothiazine type MDR modulators.

Experimental

Compounds and activity data

The investigated phenothiazines and structurally related compounds are shown in Table 1. The ability of a compound to ameliorate MDR was evaluated by Ramu and coworkers[12] by comparing the ED_{50} values obtained in P388/ADR cells incubated in the absence versus the presence of 0.2 μM ADR. This ADR dose was just below the concentration that produced a detectable growth-inhibitory effect on these cells.[12]

QSAR methods

The Free–Wilson analysis (Fujita-Ban modification) was applied.[22] The structures of the compounds were

coded by indicator variables for presence/absence of a given substituent at a given position and the contributions of the structural fragments to biological activity of the drugs were evaluated by multiple linear regression.

Molecular modeling methods

Molecular modeling was performed on a Silicon Graphics workstation with SYBYL 6.7 molecular modeling software.[23] Molecular mechanics (Tripos force field, Powell method, no electrostatics, 0.05 kcal/mol*A convergence criteria) and quantum chemistry method AM1 (MOPAC V 6.0) were used for geometry optimization and calculations of the atomic charges. CoMFA and CoMSIA were used for 3D-QSAR analysis. Default characteristics of the grid region and the carbon probe atom were used. Steric, electrostatic and both CoMFA fields were calculated. The standard energetic field cut-off value of 30 kcal/mol with no electrostatic interactions at bad steric points was used. Preliminary investigations indicated no significant influence of the threshold column filtering σ_{min} therefore the defaut σ_{min} of 2 kcal/mol was used. CoMSIA calculations were done with a defaut attenuation factor 0.3. Steric, electrostatic, hydrophobic and hydrogen-bond donor and acceptor similarity indices were calculated.[24]

Calculation of physicochemical properties

ACD/Labs V 5.0 software was used to calculate pKa and log$P$ values.[25] 'Apparent constants' method for pKa calculation was used. The algorithm automatically protonates the sketched-in molecule by 'adding' protons to the molecule in order in which the molecule would normally be protonated in solution. The method was chosen as it mimics the experimental situation in solution.

Statistical methods

Multiple linear regression in STATISTICA V5.0 was used in the Free–Wilson analysis. Each model was estimated by correlation coefficient, R^2, standard error of estimate *SEE*, and the *F*-value. The CoMFA and CoMSIA QSAR equations were derived by the PLS method. The leave-one-out cross-validation procedure was applied. The models were estimated by the cross-validated R^2, Q^2_{cv}, the optimal number of components, N_{opt}, and the standard error of prediction, SEP_{cv}. The optimal number of components, N_{opt}, corresponded to maximum Q^2_{cv}. Noncross-validated models (characterized by the correlation coefficient, R^2, standard error of estimate, *SEE*, and *F*-value) were obtained with N_{opt}. The models were validated by prediction of test compounds using the models obtained by noncross-validation with N_{opt}. The predictive R^2, Q^2_{pr}, was calculated for the test set compounds using the equation: $Q^2_{pr} = (SD - PRESS)/SD$, where $SD = \Sigma (Y_{act} - Y_{mean})^2$ and $PRESS = \Sigma(Y_{act} - Y_{pred})^2$. Y_{act} and Y_{pred} are the actual and predicted activities, respectively, of the test set compounds and Y_{mean} is the mean activity of the training set compounds.

Geometry optimization and alignment of molecules

The local energy minimum structures of some compounds (numbers **1**, **2**, **3**, **11**, **12**, **18**, **21**, **24** and **25** in Table 1) as obtained in[14] were used and the remaining structures were built from them. The starting geometries were optimized by Tripos force field, keeping the tricyclic ring system as an aggregate, and the final optimization was done with AM1 semiempirical method using the key words 'Precise' and 'XYZ'. The optimized structures were superimposed by the RMS fit alignment technique. The so called 'shape' alignment was used by fitting the centroids of the two aromatic rings in the tricyclic system and the first tertiary nitrogen in the aliphatic chain.[14] Two types alignment of the monoprotonated forms were used. The first one involved the centroids of the aromatic rings and the first nitrogen in the aliphatic chain without considering its protonation state. This alignment was coded as alignment 1 and resembled the alignment of the neutral forms. The second one was based on the centroids of the two aromatic rings and the protonated nitrogen atom in the aliphatic chain according to the calculated pKa values (Table 1). It was coded as alignment 2.

References and Notes

1. Gottesman, M.; Pastan, I. *Annu. Rev. Biochem.* **1993**, *62*, 385.
2. Safa, A. In: *Methods in Enzymology*; Ambudkar, S.; Gottesman, M., Ed.;. Academic: San Diego, 1998; Vol. 292, pp. 289–307.
3. Ford, J.; Hait, W. N. *Pharmacol. Rev.* **1990**, *42*, 155.
4. Kellen, J. *Anticancer Res.* **1993**, *13*, 959.
5. Ford, J. M. *Hematol./Oncol. Clin. North Am.* **1995**, *9*, 337.
6. Ambudkar, S.; Dey, S.; Hrycyna, C.; Ramachandra, M.; Pastan, I.; Gottesman, M. *Annu. Rev. Pharmacol. Toxicol.* **1999**, *39*, 361.
7. Ahkmed, N.; Fojo, A. T.; Bates, S. E.; Scala, S. *Proc. Am. Assoc. Cancer Res.* **1995**, *36*, 339.
8. Chiba, P.; Ecker, G.; Schmid, D.; Drach, J.; Tell, B.; Goldenberg, S.; Gekeler, V. *Mol. Pharmacol.* **1996**, *49*, 1122.
9. Ford, J. M.; Prozialeck, W. C.; Heit, W. N. *Mol. Pharmacol.* **1989**, *35*, 105.
10. Ford, J. M.; Briggeman, E. P.; Pastan, I.; Gottesman, M.; Hait, W. N. *Cancer Res.* **1990**, *50*, 1748.
11. Ramu, A. In: *Resistance to Antineoplastic Drugs*; Kessel, D., Ed., CRC: Boca Raton, Florida, 1989, pp 63-80.
12. Ramu, A.; Ramu, N. *Cancer Chemother. Pharmacol.* **1992**, *30*, 165.

13. Pajeva, I.; Wiese, M. *Quant. Struct.–Act. Relat.* **1997**, *16*, 1.

14. Pajeva, I.; Wiese, M. *J. Med. Chem.* **1998**, *41*, 1815.

15. Pajeva, I.; Wiese, M. *Quant. Struct.–Act. Relat.* **1999**, *18*, 369.

16. Tmej, C.; Chiba, P.; Huber, M.; Richter, E.; Hitzler, M.; Schaper, K.-J.; Ecker, G. *Arch. Pharm. Pharm. Med. Chem.* **1998**, *331*, 233.

17. Kim, K. *Bioorg. Med. Chem.* **2001**, *9*, 1517.

18. Ecker, G.; Huber, M.; Schmied, D.; Chiba, P. *Mol. Pharmacol.* **1999**, *56*, 791.

19. Higgins, C. F. *Cell* **1994**, *79*, 393.

20. Stein, W. D. *Physiol. Rev.* **1997**, *77*, 545.

21. Schmid, D.; Ecker, G.; Kopp, S.; Hitzler, M.; Chiba, P. *Biochem. Pharmacol.* **1999**, *58*, 1447.

22. Kubinyi, H. In: *Comprehensive Medicinal Chemistry*; Sammes, P.; Taylor, J., Ed.; Pergamon Press: Oxford, 1990; Vol. 21, pp 593–610.

23. Tripos Inc., 1699 Hanley Road, St. Louis, MO 63144, USA.

24. Klebe, G. In: *3D-QSAR in Drug Design. Recent Advances*; Kubinyi, H.; Folkers, G.; Martin, Y., Ed.; Kluwer/ESCOM: Dordrecht, 1998; Vol 3, pp 87–104.

25. Advanced Chemistry Development Inc., 90 Adelaide Street West, Suite 702, Toronto, Ontario M5H 3V9, Canada.